We are IntechOpen, the world's leading publisher of Open Access books Built by scientists, for scientists

6,900
Open access books available

185,000
International authors and editors

200M
Downloads

Our authors are among the

154
Countries delivered to

TOP 1%
most cited scientists

12.2%
Contributors from top 500 universities



WEB OF SCIENCE™

Selection of our books indexed in the Book Citation Index in Web of Science™ Core Collection (BKCI)

Interested in publishing with us?
Contact book.department@intechopen.com

Numbers displayed above are based on latest data collected.
For more information visit www.intechopen.com



Chapter 20

YSZ Reinforced Ni-P Composite by Electroless Nickel Co-Deposition

Nor Bahiyah Baba

Additional information is available at the end of the chapter

http://dx.doi.org/10.5772/46496

1. Introduction

The importance of nickel ceramic composite in engineering applications especially for corrosion (Rabizadeh and Allahkaram 2011), wear (Lekka, Zanella et al. 2010) and thermal (Gengler, Muratore et al. 2010) resistance, and also for fuel cell anode (Pratihar, Sharma et al. 2007) has increasingly significance. Nickel ceramic composite namely Ni-P-YSZ manufactured by electroless nickel (EN) co-deposition process is investigated for its composite ratio, porosity content and electrical conductivity. The composite is the state-of-the-art as it is the combination of nickel that is very well known for its high thermal, electronic conductivity and corrosion resistance with yttria-stabilised zirconia (YSZ) for its high ionic conductivity, impact and hardness strength. The understanding of this composite formulation and properties will increase its ability as well as expanding its application in multi-engineering disciplines.

The unique of this composite is the fabrication method via EN co-deposition process. This is a single fabrication method consists of an in-situ incorporation of inert ceramic particles in the conventional Ni-P matrix. The co-deposition of fine particle in-situ in an electroless metal-matrix is very attractive as it saves energy and time. Typical co-deposition consists of particulates in the size range of 0.1-10 μm with loading of up to 40 vol.% of the total matrix (Feldstein 1990). Common fabrications for particulate composites are limited to conventional ceramic processing, solid state powder processing and thermal spraying techniques. The incorporation of particles in EN deposit has been widely investigated and the application of ceramic YSZ in EN composite coating is the new approach (Baba, Waugh et al. 2009).

EN deposition is an autocatalytic electrochemical reaction by a chemical reduction of nickel ions near the surface of the activated substrate (Feldstein 1990). In addition to its good coating characteristics, this process can be applied to the surfaces of almost all materials. The understanding of EN chemical process as described by equations (1) - (4) is the key to

INTECH
open science | open minds

© 2012 Baba, licensee InTech. This is an open access chapter distributed under the terms of the Creative Commons Attribution License (http://creativecommons.org/licenses/by/3.0), which permits unrestricted use, distribution, and reproduction in any medium, provided the original work is properly cited.

control the EN deposition morphology, composition and properties. The conventional EN deposition processes are a direct chemical reduction of nickel ions from EN Slotonip 1850 (Schloetter 2006) solution to metallic nickel process as illustrate in equation (2) and the deposition of phosphorus in equation (3) below. This process is controlled by the EN bath composition, bath temperature, bath pH and soaking time, deposition rate, substrate surface and substrate orientation. Altering the process parameters cause physical changes to the deposit.

$$(H_2PO_2)^- + H_2O \rightarrow H^+ + (HPO_3)^{2-} + 2H_{abs} \cdots \quad (1)$$

$$Ni^{2+} + 2H_{abs} \rightarrow Ni + 2H^+ \cdots \quad (2)$$

$$(H_2PO_2)^- + H_{abs} \rightarrow H_2O + OH^- + P \cdots \quad (3)$$

$$(H_2PO_2)^- + H_2O \rightarrow H^+ + (HPO_3)^{2-} + H_2 \cdots \quad (4)$$

The application of EN deposition in producing composites by in-situ incorporation of inert particles in the conventional Ni-P matrix has been extensively researched, i.e. incorporation of diamond, silicon carbide, silicon nitride, silicon oxide, boron carbide, alumina, iron oxide, titanium oxide, ceria, yttria, zirconia and PTFE particles with varying the particulate sizes (micro or nano), as listed in Table 1.

The composition of nickel and YSZ must be controlled to result in the desired properties. High ceramic composition ensures high wear, thermal and corrosion resistance. At the same time, the coefficient of thermal expansion within the coating and between coating and substrate should be compatible to avoid cracking and delamination respectively. Finally, the proportion of ceramic YSZ coating in the composite can be varied from layer to layer. The construction of a gradient of coating layers, for example, with lower ceramic content inside, at the lowest layer, increasing through subsequent layers confers the advantages of heat and corrosion resistance.

In order to effectively control the composition of Ni-YSZ composites for the best results, the conventional EN deposition process must be understood in terms of the process parameters especially the EN bath chemical and substrate conditions that affect its efficiency and quality. In addition to bath composition, conventional EN deposition is also controlled by several other bath-related factors such as bath temperature, bath pH and soaking time (Baudrand 1994).

The properties and affecting factors of conventional EN deposition might or might not be applicable to EN co-deposition. A study showed that the structural characteristics and phase transformation of EN co-deposition incorporating Si_3N_4, CeO_2 and TiO_2 remained unchanged as from those of the conventional EN deposition. In general, various factors have been shown to affect the deposition of EN composites, including (1) particle catalytic inertness, (2) particle charge, (3) EN bath composition, (4) bath reactivity, (5) particle compatibility with the matrix, (6) plating rate, and (7) particle size distribution (Feldstein 1990).

Types	Particle	Molecular formula	References
Inert/ hard materials	Diamond	C	(Hung, Lin et al. 2008); (Matsubara, Abe et al. 2007); (Sheela and Pushpavanam 2002)
	Silicon nitride	Si_3N_4	(Balaraju and Rajam 2008); (Dai, Liu et al. 2009); (Das, Limaye et al. 2007)
	Silicon carbide	SiC	(Berkh, Eskin et al. March 1996); (Kalantary, Holbrook et al. 1993); (Lin, Chen et al. 2006)
	Silicon oxide	SiO	(Dong, Chen et al. 2009)
	Boron carbide	B_4C	(Vaghefi, Saatchi et al. 2003)
	Alumina	Al_2O_3	(Balaraju, Kalavati et al. 2006); (Hazan, Reutera et al. 2008; Hazan, Werner et al. 2008)
	Ceria	CeO_2	(Necula, Apachitei et al. 2007)
	Yttria	Y_2O_3	(McCormack, Pomeroy et al. 2003)
	Zirconia	ZrO_2	(Shibli, Dilimon et al. 2006)
	Iron oxide	Fe_30_4	(Zuleta, Galvis et al. 2009)
Others	Polytetrafluoroethylene	PTFE	(Ger and Hwang 2002)
	Titanium oxide	TiO_2	(Balaraju, Narayanan et al. 2006)
Multiple	Silicon carbide- Alumina	$SiC-Al_20_3$	(Li, An et al. 2005; Li, An et al. 2005; Li, An et al. 2006)
	Silicon carbide-Graphite	SiC-G	(Wu, Shen et al. 2006)
	Silicon carbide- PTFE	SiC-PTFE	(Huang, Zeng et al. 2003)
	Zirconia-Alumina- Zirconium aluminide	ZrO_2-Al_2O_3-Al_3Zr	(Sharma, Agarwala et al. 2005)

Table 1. Types, names and formulas of the particles used in EN co-deposition

Particle stability in this case could be the charge stability of the particles in the solutions. Particle stability determines the particle dispersion in the solution and particles' tendency for agglomeration or sendimentation. Necula et al. (2007) found that particles are having good dispersion stability in deionised water but not so in the EN solution. Studies on alumina (Hazan et al. 2008b, 2008a), boron carbide (Vaghefi et al. 2003) and ceria (Necula et al. 2007) particles showed that the dispersion stability strongly depends on pH and the low stability caused a short sedimentation time. Studies by Hazan et al. (2008b; 2008a) on dispersion stability in Ni-P-Al_2O_3 EN system incorporating comb-polyelectrolyte showed high particle concentrations of up to 50 vol.% particle incorporation.

Periene et al. (1994) concluded that volume percent of co-deposition particles is dependent on powder conductivities and hydrophobic/ hydrophilic properties. Another study done on

co-depositing boron carbide (B_4C) with particle sizes ranging from 5 to 11 μm in hypophosphite-reduced EN solution gave a maximum of 33 vol.% B_4C when the B_4C particles were wetted with surfactant before being added into the bath (Vaghefi, Saatchi et al. 2003). The surfactant is a blend of surface active agent which contains both hydrophilic and hydrophobic groups which helps increase deposition, even at 8 gl^{-1} particle loading. The application of surfactant in the deposition of PTFE on low carbon steel substrate showed strong adsorption (Ger and Hwang 2002).

The shape and size of the particles play an important role as they influence the deposition surface area and energy. It was found that spherical particles with smaller particle size (average 1 μm boron particles and 3.4 μm alumina particles) gave high particle concentration in the matrix (Apachitei, Duszczyk et al. 1998). Study done Balaraju et al. (2006a) varying alumina powder sizes of 50 nm, 0.3 μm and 1.0 μm showed that the highest particle incorporation occurred at 1.0 μm particle size.

Another important factor is the particle loading. Particle loading is the amount of powder particles in a litre solution. Co-depositing very fine polycrystalline diamond ranging between 8 and 12 μm with varying concentrations from 2-10 g/l onto aluminium substrate at 70-90°C for an hour yielded as high as 18.40 vol.% diamond powder in the deposit (Sheela and Pushpavanam 2002). The particle incorporation in a Ni-P-ZrO_2 EN system was found to be directly proportional to increase particle loading up to 9 g/l as well as the deposition rate (Shibli, Dilimon et al. 2006). In Ni-P-B_4C EN system, particle composition in the matrix increased from 12 to 33 vol.% as the particle loading increased from 1 to 8 g/l (Vaghefi, Saatchi et al. 2003). It was found that a particle loading more of than 15 g/l SiC in hypophosphite-reduced solution caused extensive bath foaming which reduced the plating rate (Kalantary, Holbrook et al. 1993).

Bath conditions might be disturbed by the addition of inert particles. The addition of silicon carbide (SiC) powders with particle size ranging from 4-7 μm in varying EN solution conditions (composition, pH, temperature and time) showed an increase in SiC loading in the deposition but a reduction of the deposition rate and deposition weight (Kalantary, Holbrook et al. 1993). Another study showed that co-deposition of SiC (1-5 μm) in sodium hypophosphite-reduced EN solution at pH 4.5-5.5, 80-90°C with air agitation resulted in 25-30 vol.% SiC in the deposition (Li 1997). Aggressive agitation might cause substrate or deposition abrasion by other factors such as particle hardness, particle shape and size, particle loading and bath movement (Kalantary, Holbrook et al. 1993).

Substrate orientation is defined as the position of the substrate in the EN bath during the EN deposition. The variations of substrate position have shown to give an effect on the EN deposition. In a study by Sheela & Pushpavanam (2002) on diamond EN co-deposition in hypophosphite-reduced solution showed that a vertical substrate position gave less than 20% particle incorporation compared to the horizontal position. Another study on Ni-P-SiC using hypophosphite-reduced solution with a particle loading of 25 g/l showed that the substrate held tangentially gave the highest particle composition in the matrix and a vertical

position leading to uniform particle incorporation and adherence provided, that uniform agitation was used (Kalantary et al. 1993).

Having discussed all the above affecting factors on EN co-deposition process, the study is concentrated on four of the factors, namely, particle size (Balaraju, Kalavati et al. 2006), agitation method (Sevugan, Selvam et al. 1993), bath pH (Liu, Hsieh et al. 2006), and substrate surface treatment (Teixeira and Santini 2005). The application of design of experiment (DoE) using full factorials of a two-level factor is economical and practical to reduce the number of experiments. Unlike the Taguchi method, full factorial DoE highlights the significant main and interactions effects between the factors (Anthony 2003).

Factorials design is the basis of DoE. Factorials design is the most efficient way to study the effects of two or more factors. For example, 2-levels is simplified as 2^k or three levels as 3^k. Factorial design investigates all possible combinations of factor levels for each complete trial or replication of experiment. This is because the factors arranged in a factorial design are crossed by the Yates algorithm (Bisgaard 1998). A 2^k factorial design is used to study the effects of k factors with two levels for each factor. The k represents a multiple-factor design with a variation of treatment designs where a set of treatments (*factors*) are tested over one or more sets of treatments (*levels*). In practice the higher-order interactions are usually not significant, thus most design are limited to 2-3 levels.

The effects of EN composite coating parameters on Ni-YSZ composition and porosity content were investigated and optimized using full factorials and ANOVA. An empirical model for prediction of Ni composition and porosity content were established by means of piecewise linear regression analysis. The composite response to electrical conductivity is also investigated.

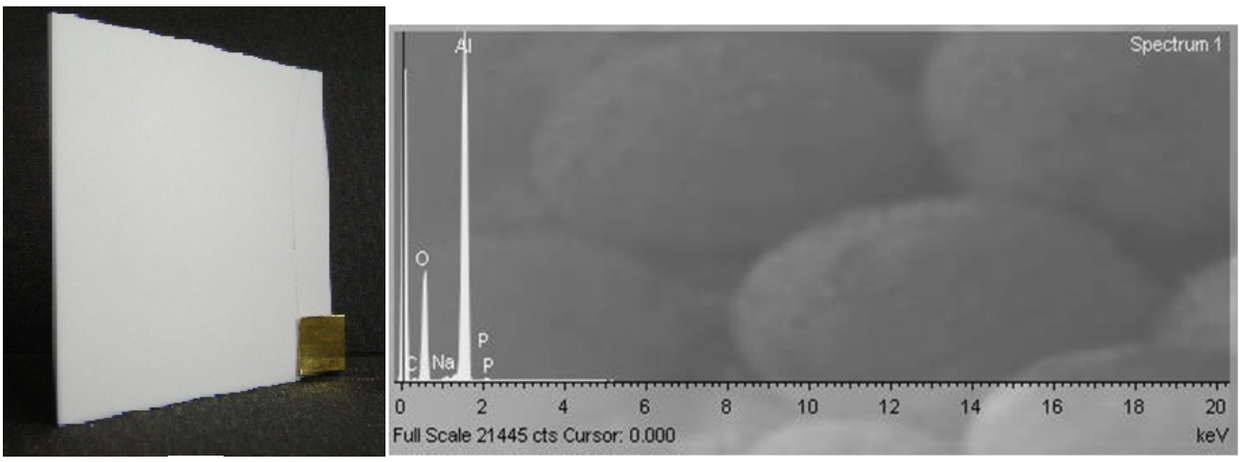
2. Experimental methods

2.1. Materials and preparations

A ceramic substrate of alumina tile (Coors Ceramics, U.K.) with manufacturer standard dimensions of 50 x 50 x 1 mm as shown in Figure 1 was used as the base for composite deposition. Surfaces of the substrate sample were treated by chemical etching and mechanical blasting. Chemical etching of the substrate sample was done by immersion for 5 minutes at room temperature in a hydrofluoric (HF) etching solution comprising a mixture of 1 part hydrofluoric acid (20ml/l) to 5 parts ammonium fluoride (NH_4F) (2g/l). Then mechanical treatment of the substrate was done by blasting the substrate with brown alumina sand for 1-2 minutes. The contamination after sand blasting was cleaned ultrasonically for 30 minutes at room temperature by submerging the substrate samples individually in beakers filled with acetone.

Reinforcement ceramic particles of 8 mol% YSZ (8YSZ; United Ceramics, England) were used. Yttria stabilised zirconia (YSZ) is a ceramic phase that is very well-known for high hardness, good scratch and corrosion resistance; and very high thermal resistance, but low

toughness and high brittleness. Normally the addition of ceramic particles in composites increases the composite's mechanical properties in term of its hardness, corrosion resistance and thermal resistance. The 8YSZ particles varied between the nominal sizes of 2 μm and 10 μm.



(a) (b)

Figure 1. (a) Alumina tile as a ceramic substrate for EN co-deposition (b) Alumina substrate EDX spectrum

2.2. EN co-deposition

The ceramic alumina substrate requires sensitising to activate the surface. All non-proprietary solutions were prepared using AR grade chemicals and high purity deionised water. After the pre-treatment process sequence as listed in Table 2, the EN composite deposition of Ni-YSZ was performed within 3 hours to minimize effects of chemical degradation. The EN chemicals produced a bright mid-phosphorous (6 – 9%) nickel deposit. The solution was heated and the temperature maintained at 89^{o}C using a Jenway hotplate.

Trade name	Soaking Time	Temperature
Cuprolite X96DP	15 min	60^{o}C
Uniphase PHP Pre-catalyst	15 min	20^{o}C
Uniphase PHP Catalyst	15 min	40^{o}C
Niplast AT78	15 min	40^{o}C
Electroless Nickel SLOTONIP 1850	60 min	89^{o}C

Table 2. EN co-deposition materials and procedure

A ceramic powder of 50g/l was added into the bath along with the substrate. With agitation, suspended particles near the surface are co-deposited onto the substrate surface. The pH of the EN solution was varied between the manufacturer standard pH 4.9 and pH 5.4. The pH was altered to pH 5.4 by adding 10% ammonium hydroxide. The coating time was kept constant at 60 minutes. The bath temperature was kept constant at 89 ± 2^{0}C. The particles

were kept in suspension in the EN bath by either mechanical stirring or air bubbling agitation methods. Mechanical stirring was done by Jenway hotplate with magnetic stirrer, and air bubbling was performed at1.2W air pressure.

2.3. SEM-EDX

Composition of Ni-P and YSZ composite in the deposition is controlled to give desired properties. It is desirable to get high ceramic to metal ratio for corrosion, thermal and wear resistance and even in the application of anode of fuel cell. Varying ceramic YSZ deposition in the composite has an advantage in which a gradient of coating layers with increasing ceramic content inside to outside for heat and corrosion resistance respectively. The influence of the process parameters in gaining high particle incorporation is analysed. The characterisation of the composite deposition was done by Hitachi field emission gun scanning electron microscope (SEM) coupled with energy dispersive x-ray (EDX).

The common setting of SEM is 24 mm working distance and 25 kV acceleration voltage unless stated otherwise to ensure optimum condition for EDXA. Magnification at 1000 or 2000 and resolution are varied according to the requirement (3.9-6.0). The EDX expose time was kept constant at 300s and expose area was kept constant throughout the whole specimens.

SEM enables surface morphology and chemical microanalysis in conjunction with EDX. EDX stands for Energy dispersive X-ray where an x-ray emitted during electron beam targeted to the sample surfaces is detected and collected for elemental composition characterisation. The electron beam bombardment knock-out the electron near the surface and resulting electron vacancy is filled by higher energy electron level. This energy is between 10-20 eV, depending on the materials and emits x-rays to balance the energy difference between the two electron states. EDX collaborated with INCA software extends its ability for quantitative analysis, qualitative analysis, elemental mapping, and line profile analysis.

2.4. Archimedes buoyancy

Archimedes specific density can be used to measure the porosity fraction in a material. The basic Archimedes principle states that the amount of displaced water volume is equal to the immersed object volume. The determination of the solid substance density can be done by buoyancy or displacement methods. The true density on the other hand is the total solid density. Figure 2 (Sartorius 1991) illustrates the Archimedes density buoyancy methods. The density of a solid body is defined as a product of fluid density and fraction of solid mass over fluid mass. The apparent weight of a body in a liquid – weight reduced by buoyancy force is measured. The density of water at room temperature is assumed to be unity. The substrate alumina tile is assumed to be fully dense thus the calculation of pores of deposition will not be affected by the substrate.

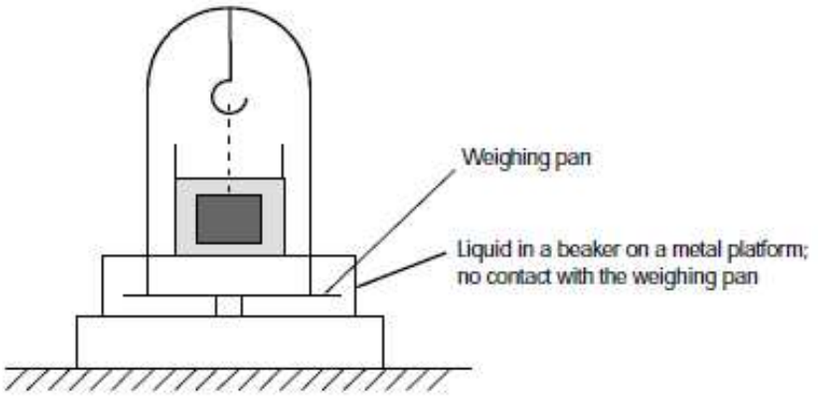


Figure 2. Schematic diagram of Archimedes density buoyancy measurement (Sartorius 1991)

2.5. Four-point probe

The composite fabricated via EN co-deposition was tested in term of its electrical resistivity and conductivity performance measured using four-point probe. The conductivity performance of the Ni-YSZ composite was tested in air environment up to 800°C. Then another set of test where the nitrogen gas was purged into the furnace up to 600°C at 20°C/min. A four-point probe was used to measure the sheet resistance and thus the resistivity and conductivity of the anode at every 5-15°C increment under 50 mA current.

The resistance of Ni-YSZ anode was measured using four-point electrical probe as illustrate in Figure 3. A power supply provides a constant current flow between probe 1 and 4. The current output can be obtained by an ammeter. The second set of probe (probe 2 and 3) is used for sensing and since negligible current flows in these probes – only voltage drop – thus accurate resistance is measured. A resistance of the sample between probes 2 and 3 is the ratio of the voltage registering on the digital voltmeter to the value of the output current of the power supply. A simple 4-point measurement at room temperature was done at 1 mA, 50 mA and 90 mA at two different points as a trial test.

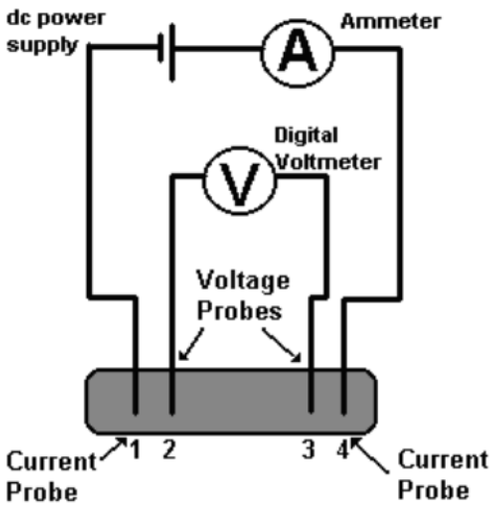


Figure 3. Schematic four-point probe set up

2.5. Full factorials

As for the EN composites process, the conventional process is disturbed by the addition of 8 mol% YSZ (8YSZ; United Ceramics, England) particles in the bath. Therefore the co-deposition process is not only affected by the basic process parameters but also other factors including the particle stability, particle size and shape, particle loading, and bath agitation (Feldstein 1990). Few process parameters were identified to be most effective in gaining the yields namely bath agitation, bath pH, particle size and surface treatment. These parameters were then design for experiment using 16 run full factorials with five replications.

The experimental design involved four EN co-deposition process parameters (Table 3). Both EN conventional and composite coating have been shown to be very much affected by bath pH, bath agitation, substrate surface condition, and by particle shape and size in the composite EN coating. A full factorials DoE approach with four parameters at two levels gave 2^4 full factorials of 16 runs. The DoE was repeated five times independently yielding 80 sets of experimental data.

Parameters	Symbols	Level	
		Low (-1)	High (+1)
Particle size	A	2	10
Bath agitation	B	Air Bubbling	Mechanical Stirring
Bath pH	C	4.9	5.4
Surface treatment	D	HF Etching	Mechanical Blasting

Table 3. EN co-deposition process parameters and their levels

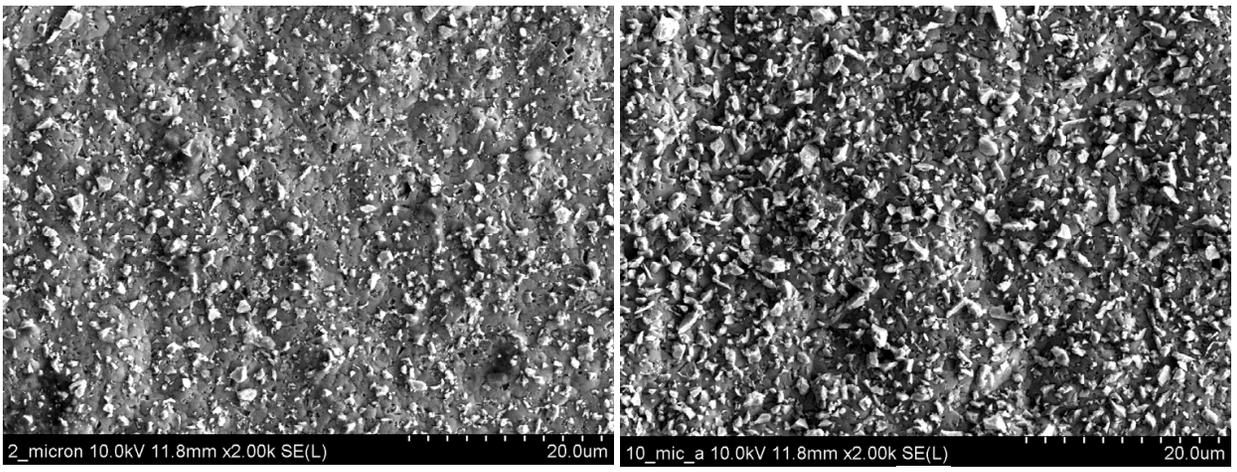
3. Results and discussions

3.1. Composite characterisation

Ni-YSZ was successfully deposited on alumina substrate by EN co-deposition. The typical microstructure of EN Ni-YSZ composite deposition is shown in Figure 4. The ceramic co-deposition of 10 microns (Figure 4b) ceramic powders in EN Ni-YSZ composite is higher compared to the 2 microns (Figure 4a). The coating consists primarily of ceramic YSZ powders (white areas), metallic Ni matrix (grey areas) and pores (dark areas). In general, both coating surfaces showed uniform distribution of ceramic particles. This indicates no agglomeration of YSZ particle in the coating. Uniformly distributed ceramic particles ensure constant coefficient of thermal expansion within the coating to avoid cracking due to thermal gradient.

The corresponding EDX spectrum is given in Figure 5 shows the presence of major peak of nickel (Ni), yttria (Y), zirconium (Zr), oxygen (O) and phosphorus (P) elements with primary Kα and Lα peaks were present. These confirmed that the composites are composed of the combination of metallic nickel and ceramic YSZ. The existence of element P in the

composite is due to the fact that P is one of the major elements in the EN hypophosphite-base bath solution. The Ni-P deposition reaction in hypophosphite-based bath involved the chemical reaction as in equation (1.3) described in section 1.0.



(a) (b)

Figure 4. Comparison of surface microstructure of Ni-YSZ for ceramic particle size (a) 2 μm and (b) 10 μm

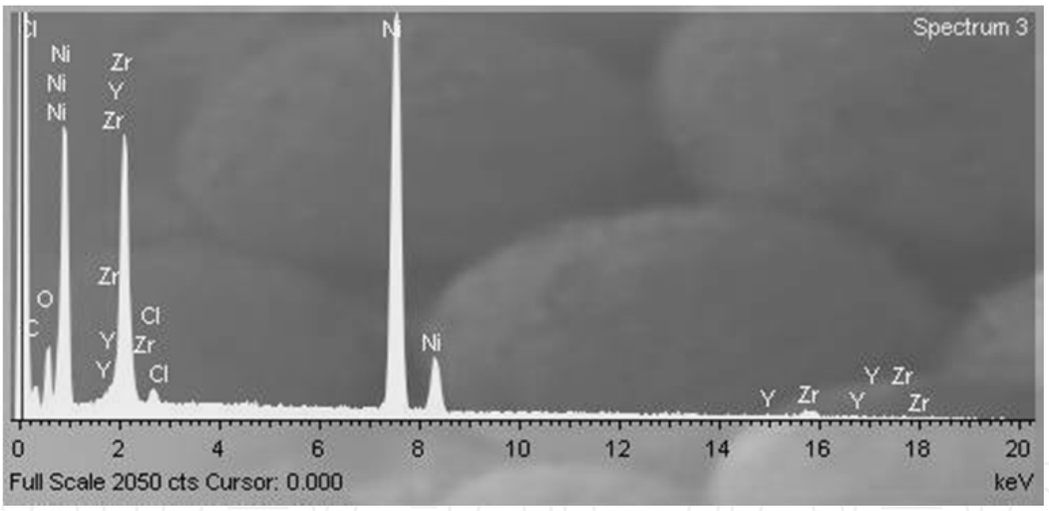


Figure 5. EDX spectrum showing presence of the corresponding EN co-deposition

In order to investigate the existence of pores at the dark areas, a higher magnification images were taken. The images show the surface morphology at various magnifications at (a) 6k, (b) 10k and (c) 20k in Figure 6. At 6k magnification image (Figure 6a) shows few dark areas which are the expected pore spots and the centre spot was focused and magnified to 10 k magnification (Figure 6b). Clearly the images confirmed the existence of pores at higher magnification of 20k (Figure 6c) the pores seemed to be open or connected.

It is expected that varying surface morphology of the substrate will increase the porosity formation. The images of field emission gun SEM at various magnifications from 1-20k are shown in Figure 7 compares the mechanical blasting treatment substrate surfaces (all images

on the left represented by a, c and e) and chemical etching treatment (all images vertically on the right represented by b, d and f). At the 1k magnification, Figure 7a (blasted) indicated more highly populated black areas compared to Figure 7b (etched). The chemically etched surface morphology is much flatter.

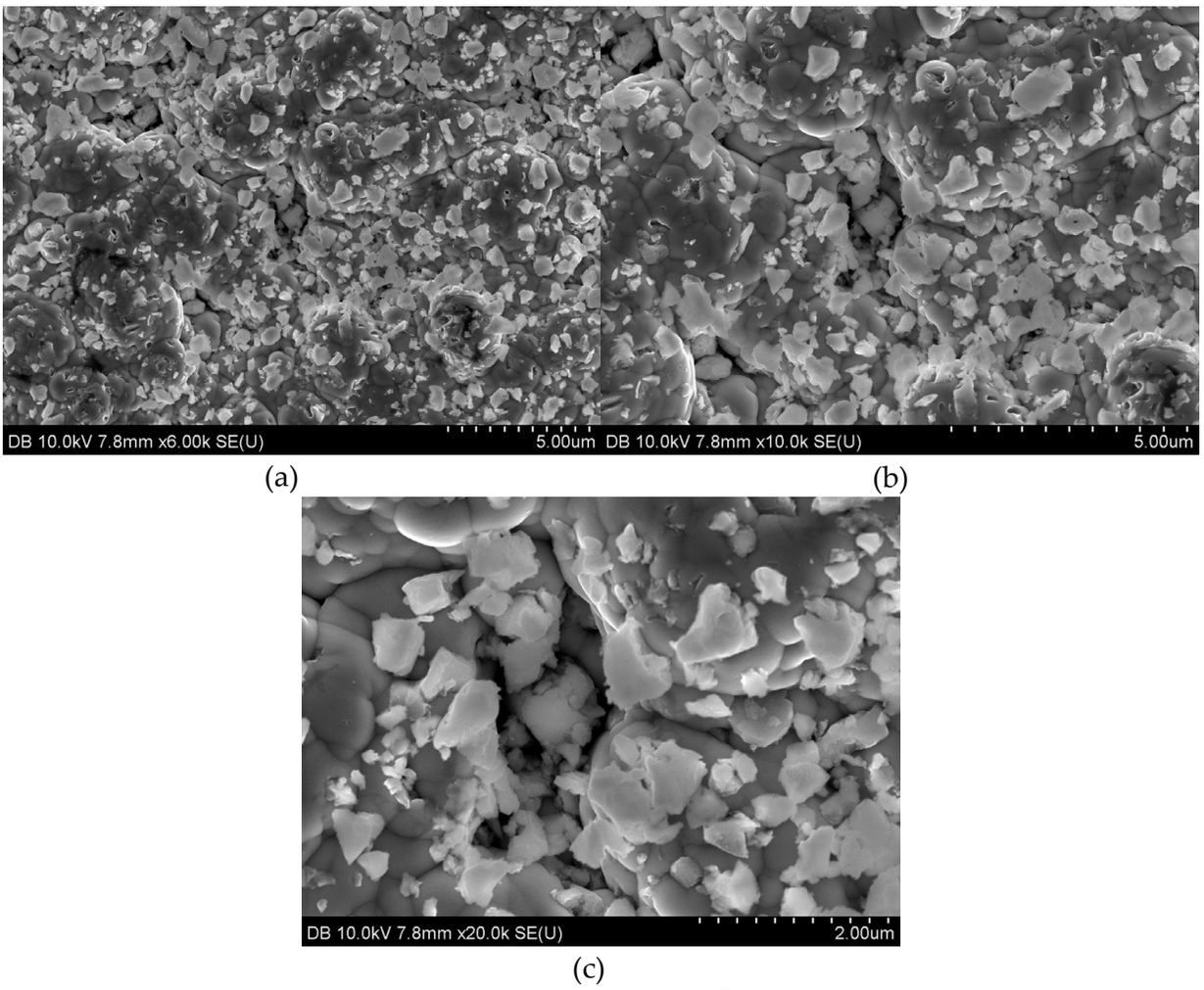


Figure 6. EN Ni- 8YSZ (2 ◎m) and bath pH5.4 at varying magnification (a) 6k (b) 10k and (c) 20k

At 5k magnification, the difference is more obvious and it is confirmed that the black areas or spots were the pores. At even higher magnification (20k), the mechanically blasted deposition (Figure 7e) exhibits many open or connected pores which are highlighted with white circles compared to the chemically etched deposition (Figure 7f).

3.2. Composite composition

Composite composition is basically an investigation of the ratio between the metallic nickel and ceramic YSZ. The composition was investigated by an analysis of the 2^k factorials design of experiment. The experiment was designed for lower nickel composition and higher ceramic incorporation in the Ni-P-YSZ composite. The main effect plot of all the four main effects namely particle size (A), agitation (B), bath pH (C) and substrate surface treatment

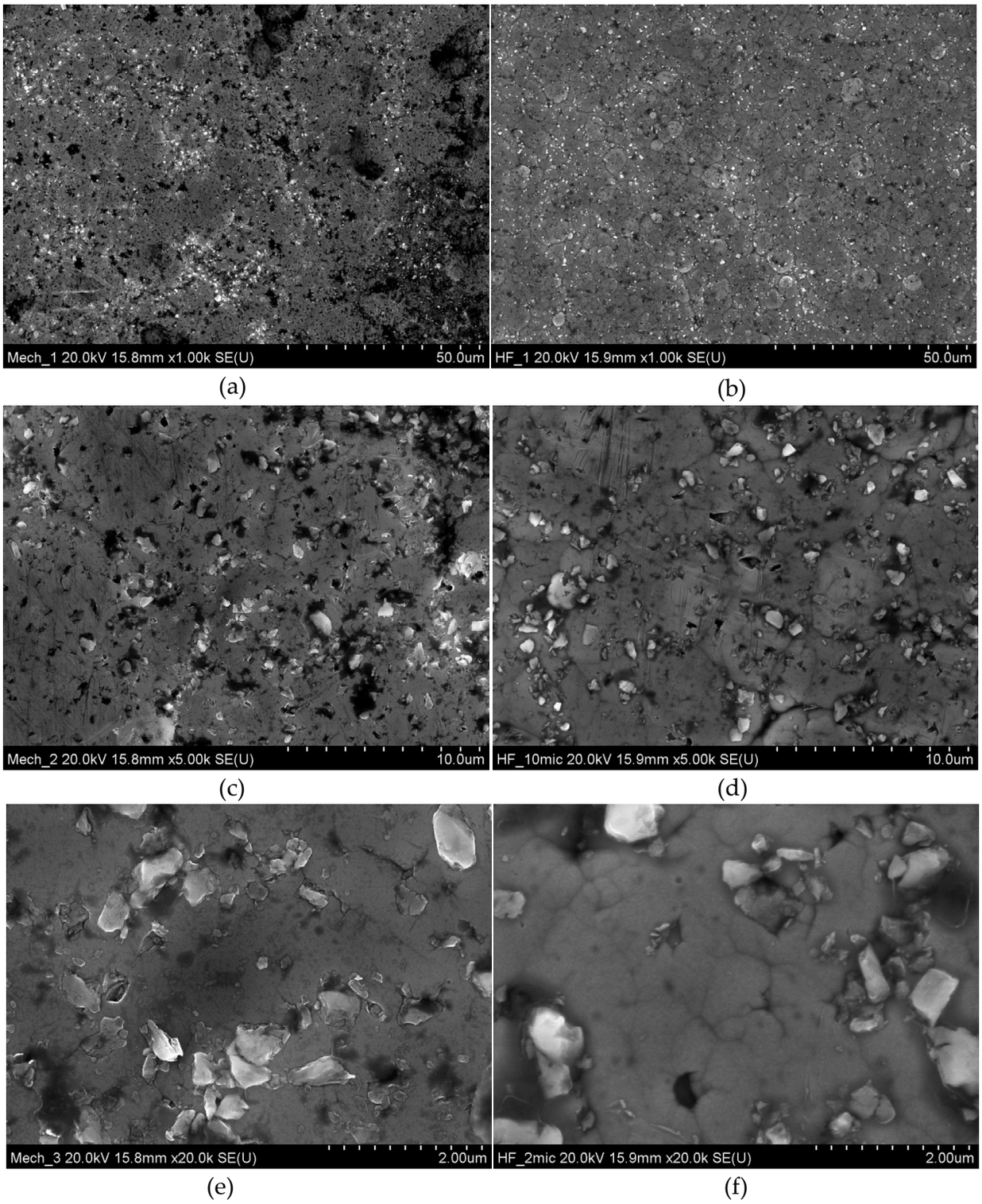


Figure 7. SEM micrographs at 1k, 5k and 20k magnification. Mechanical treated surface deposition (left: a, c, e) and chemical treated surface deposition (right: b, d, f).

(D) is illustrated in Figure 8. The main effect plot is a plot of the mean Ni content in vol.% at each level of a design parameter. The bigger the difference between the high and low levels, the higher is the effect. Referring to Figure 8, it is clearly indicated that the most significant

factor is A with 3.483 strength effects followed by C (1.341), then B (0.734) and lastly D (0.036). The effect of parameter D is almost zero, since there is almost no difference between the high and low level.

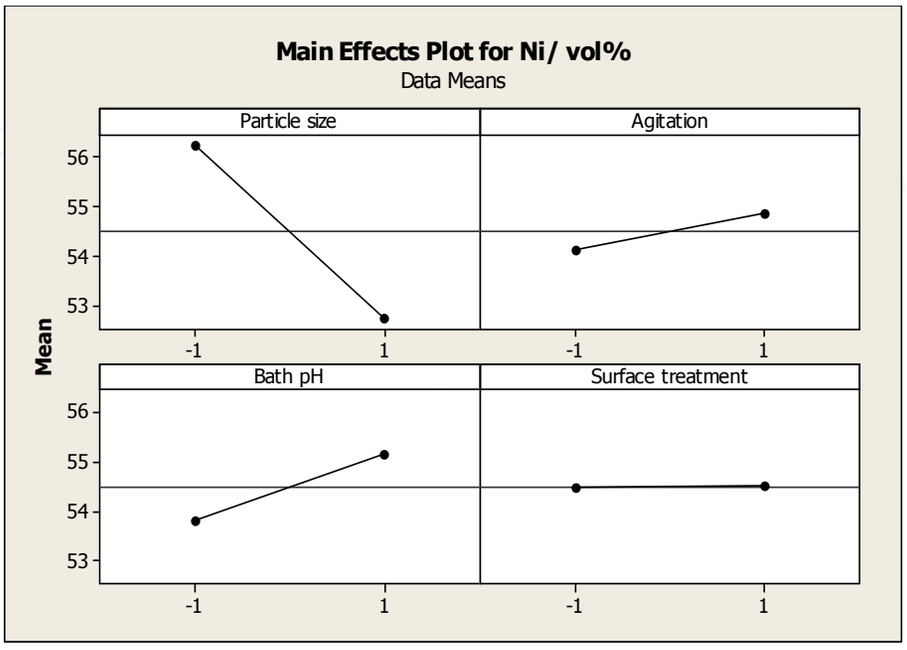


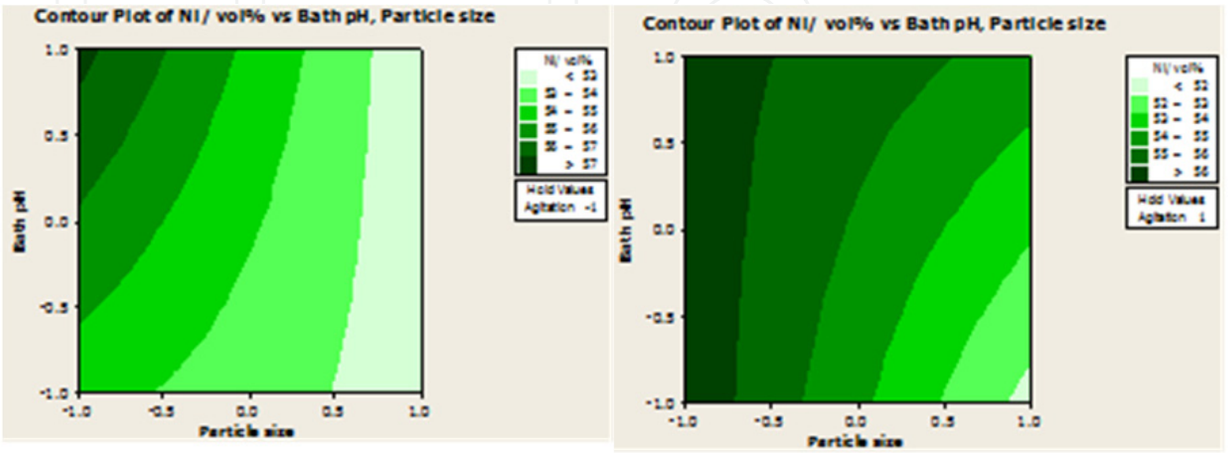
Figure 8. The main effect plots for Ni content response

Generally, by referring to the main effect plot above, particle size at high level, bath agitation at low level and bath pH at low level give the lower nickel content. This concluded that the main effects that influence the EN co-deposition process for lower Ni to YSZ deposition are particle size and bath pH. Generally, particle size (A) effect at high level (10 μm) and bath pH (C) at low level (pH 4.9) gives lower Ni to YSZ ratio.

Based on ANOVA analysis, the three-way interaction of factor A (particle size), B (bath agitation) and C (bath pH) was found to be significant. The investigation of the three-way interactions between factors A, B and C is referred to the contour plot given in Figure 9. The contour plot shows variation of the main effect factor A (particle size) and C (bath pH) where the interaction effect B (bath agitation) was kept constant at either low level of air bubbling (Figure 9a) and high level of stirring (Figure 9b). Under low level bath agitation, low Ni content was obtained at high level factor A (particle size) of 10 μm. It is also shown that factor C (bath pH) gives no effect on Ni composition at high (Figure 9a) or low level of A (Figure 9b). The low Ni content was obtained for high level bath agitation (Figure 9b) when factor A (particle size) at high level and factor C (bath pH) at low level.

The influence of factor B on both main factors A and C in determining low Ni to YSZ ratio is greatly affected by factor A (particle size). Larger particle size was found easier to be co-deposited in EN deposition rather than smaller particle size. Balaraju et. al. (2006) showed highest particle incorporation of largest alumina powder for a range of particle size between 50 nm, 0.3 μm and 1.0 μm. The lowest Ni to YSZ ratio was obtained under high level bath

agitation (mechanical stirring) with Ni content less than 52 vol.%. The effect of factor C (bath pH) on Ni content showed low level gives the lowest Ni composition in both condition of factor B. The incorporation of ceramic powders is higher under the standard EN solution pH 4.9 (Schloetter 2006) ensures optimum condition. Although higher pH increased deposition rate in conventional EN deposition (Baudrand 1994), less ceramic particles were able to be incorporated in the EN co-deposition.



(a) (b)

Figure 9. Contour plots for Ni content, pH and particle size at (a) low level agitation – air bubbling and (b) high level agitation – mechanical stirring

Thus to achieve low nickel to ceramic ratio, the conditions are (1) large particle size of 10 μm, (2) mechanical stirring agitation and (3) bath pH of 4.9. Larger particle size was found easier to be co-deposited in EN deposition rather than smaller particle size. This was supported by Balaraju et al (2006) on alumina powder sizes of 50 nm, 0.3 μm and 1.0 μm that resulted in the highest particle incorporation at 1.0 μm particle size. A study done by Vaghefi et al. (2003) showed 33 vol.% of B_4C particle with particle size ranges 5-11 μm which indicates that larger particle sizes give higher particle incorporation in the EN composite.

In terms of bath agitation, it is crucial to keep the particles in suspension throughout the deposition (Sevugan, Selvam et al. 1993). Mechanical stirring showed higher incorporation of particles in this study compared to air bubbling. It should be noted that this is in contradiction to the finding by Vaghefi (1997) in electroless nickel-phosphorus-molybdenum disulfide which showed that air purging was better than magnetic stirring. However, the particles used in this research were ceramic YSZ which, in terms of inertness, wettability and particle stability to the substrate (Apachitei, Duszczyk et al. 1998; Necula, Apachitei et al. 2007) are different to the study by Vaghefi. As for the bath pH, it is shown that a higher bath pH caused a higher deposition rate in conventional EN deposition (Baudrand 1994). Thus at a higher deposition rate, it is possible that less ceramic particles were able to be dragged along in the EN co-deposition. This resulted in the observation that the incorporation of ceramic particle is higher at lower pH of 4.9 than at 5.4.

Therefore, the best deposition parameter combination for the three-way interaction based on this observation are high level particle size of 10 um, low level bath pH of 4.9 and high level agitation of mechanical stirring (A+1B+1C-1).

3.3. Porosity content

Investigation of porosity level in the deposition is critical as the amount of porosity enhances thermal insulation for thermal barrier coatings (Wang, Wang et al. 2011) and gas circulation in fuel cell anode (Simwonis, Thulen et al. 1999) application. The amount of porosity should not be more than 40 vol.% as greater amount of porosity will reduce the mechanical properties of the deposit. Thus, an adequate amount of porosity and reasonable mechanical properties should be balance. It is known that EN deposition has excellent uniformity and dense deposition with thickness less than 10 μm (Das and Chin 1959). The amount of porosity in EN deposition could be induced by varying the agitation methods, deposition rate, bath pH and also substrate surface condition. The porosity of deposition was measured by Archimedes density measurement.

Figure 10 shows the main effect plot indicates the variation of the data mean between low and high levels for each main parameter. The most dominant parameter as already verified by the ANOVA is the substrate surface treatment (D) with bath agitation (B) closely behind. The difference between low and high levels for both parameters D and B are the largest and difficult to differentiate. Descending rank order for the strength effect is surface treatment, bath agitation, particle size and then bath pH. The 'higher-the-better' characteristic for porosity response described that high porosity content can be achieved at low level particle size (2 μm), high level bath agitation (mechanical stirring) and high level substrate surface treatment (mechanical blasting).

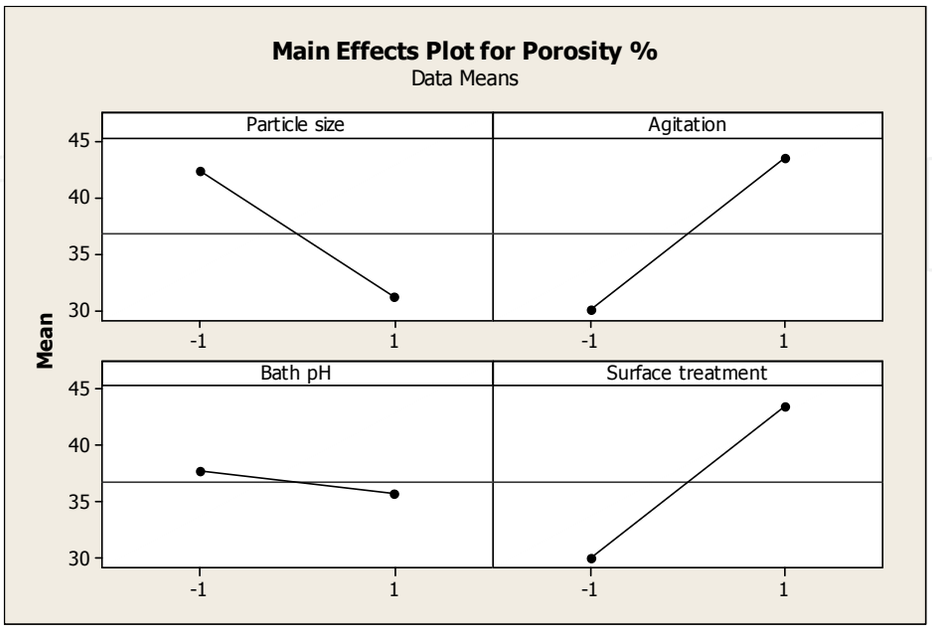


Figure 10. Main effects plot for the porosity response

The interaction plot is a powerful graphic tool which plots the mean of response of two factors. The AD interaction plot in Figure 11 shows unparallel lines of high and low level particle size under surface treatment variation. This indicates the present of interaction between the particle size and the substrate surface treatment. The porosity content was very much affected by the substrate surface treatment. Varying substrate surface treatment from low (-1) to high (+1) level increases porosity % for both particle size at low (-1) and high (+1) levels. The effect of particle size on porosity % at low level (-1) is more pronounce than at high level (+1) as the substrate surface treatment changes from low (-1) to high (+1) level. At both particle size levels, mechanical blasting gave greater effect on porosity.

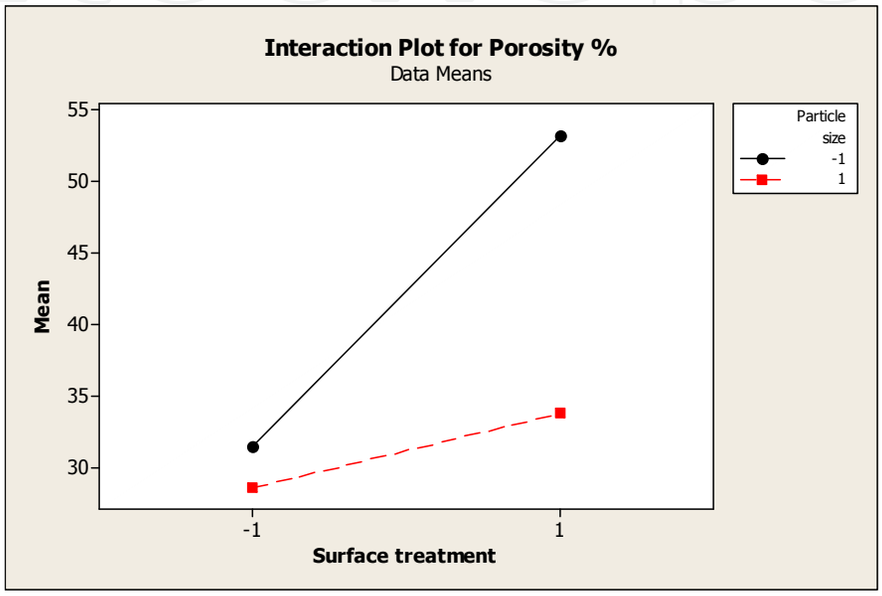


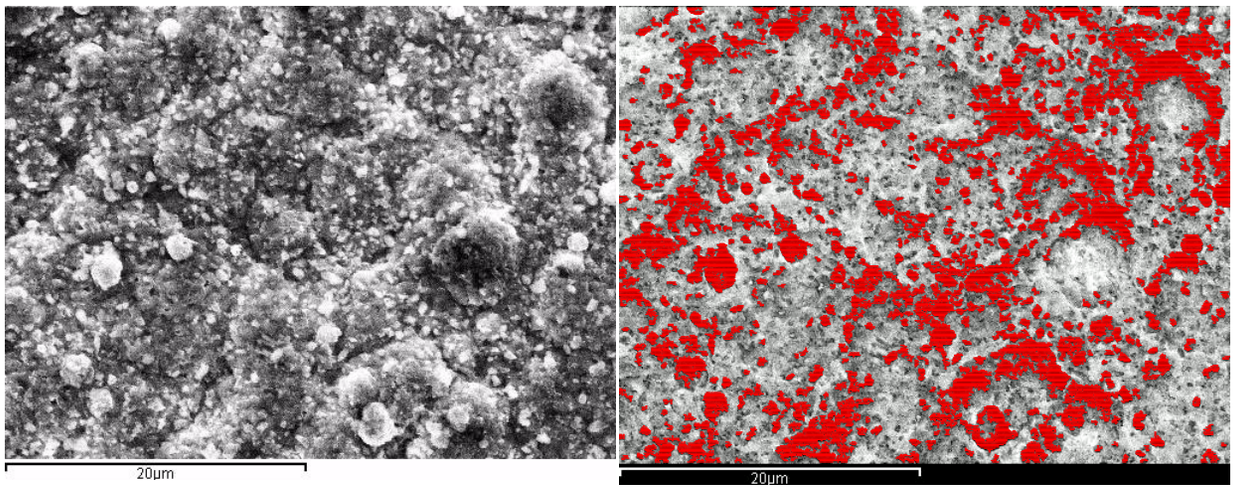
Figure 11. Figure 11: Interaction (A-D) plot for porosity

Thus to achieve high porosity content, the condition are (1) small particle size of 2 μm, (2) mechanical stirring agitation and (3) substrate surface treatment of mechanical blasting. Study by Wang et. al. (2006) has shown that fine particles introduced smaller size porosity. This indirectly indicates high porosity volume, i.e. like smaller pebbles in a jar has more quantity than the larger one. The mechanical stirring bath agitation gives higher porosity due to low removal of absorbed hydrogen or oxygen (Sevugan, Selvam et al. 1993).

The mechanical stirring bath agitation gives higher porosity as the agitation is not very aggressive compared to air bubbling thus most of the absorbed hydrogen or oxygen was not removed (Sevugan, Selvam et al. 1993) and trapped inside the EN deposition introducing more porosity. Mechanical blasting resulted in a rougher substrate surface. EN deposition is very well-known to follow the substrate profile rather than filling the spaces (Taheri, Oguocha et al. 2001). Therefore, rougher surface caused a rougher deposition surface and thus introduced more porosity.

Porosity measurement using Image Pro-Plus software was conducted. An SEM image of an EN co-deposition (8YSZ, 2 μm in bath pH 5.4) is shown in Figure 12. This image was then analysed using colour contrast for porosity measurement. The red coloured area was the

amount of porosity in the deposition (Figure 12b). It can be estimated that the coloured porosity area is approximately 20%.



(a) (b)

Figure 12. Image Pro-Plus porosity measurement; (a) SEM image (b) porosity area mapping

3.4. Regression modelling

A model to predict response function can be built by a regression model. The build model can be used to illustrate the relationship between the experimental data and the predicted data, describe the relationship between a response and a set of process parameters that affect the response. Other than that, the model can also be used to predict a response for different combinations of process parameters at their best levels. Based on the 80 sets of experimental data, the linear regression models were successfully developed for nickel to YSZ ratio response as shown in equation (5).

$$\hat{y} = 54.491 - 1.742A + 0.367B + 0.671C + 0.018D + 0.785ABC \cdots \quad (5)$$

where ŷ is the nickel content, A is particle size (µm), B is bath agitation, C is bath pH and D is surface treatment. The coefficient of determinations (R^2) was 0.72, indicating a reasonable correlation between the measured and predicted values of nickel content as shown in Figure 13. This means the model is reliable in predicting the response with 28% variation. Referring to the coefficient of the developed models, it was confirmed that particle size was the most prominent parameter in minimising the nickel to YSZ ratio.

Minitab analysis showed the optimum condition for achieving a low Ni to YSZ ratio in the coating is when factors A and B are at high level and factor C is at low level. The minimum nickel content obtained experimentally was 51.827 vol.% whereas the predicted content was 51.293 vol.%. The difference between the measured value and predicted value (0.534) is minimal, indicating that the model is reliable in predicting the response value at the desired parameter levels.

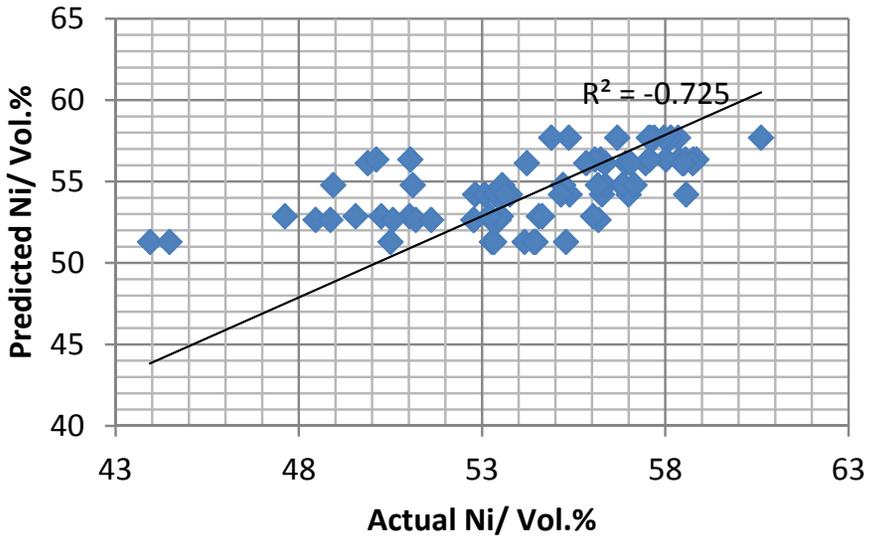


Figure 13. Comparison of experimental and predicted values of Ni content

Similarly for the Porosity %, the analysis done by Minitab in the previous section led to a reduced model that represents the optimum condition of the process in obtaining high porosity %. The reduced model equation contains main parameters A, B and D and two-way interactions of AD and is shown in equation (6).

$$\hat{y} = 36.734 - 5.614A + 6.692B + 6.776D - 4.167AD \cdots \quad (6)$$

where ŷ is the response Porosity %, A is particle size (μm), B is bath agitation and D is substrate surface treatment. The coefficient of determinations (R^2) as shown in Figure 14 is 0.47 indicating that the correlation between the actual and predicted values of Porosity % was not very good. Referring to the coefficient of the developed model, it is confirmed that the substrate surface treatment is the most prominent parameter followed by the bath pH in increasing the Porosity %.

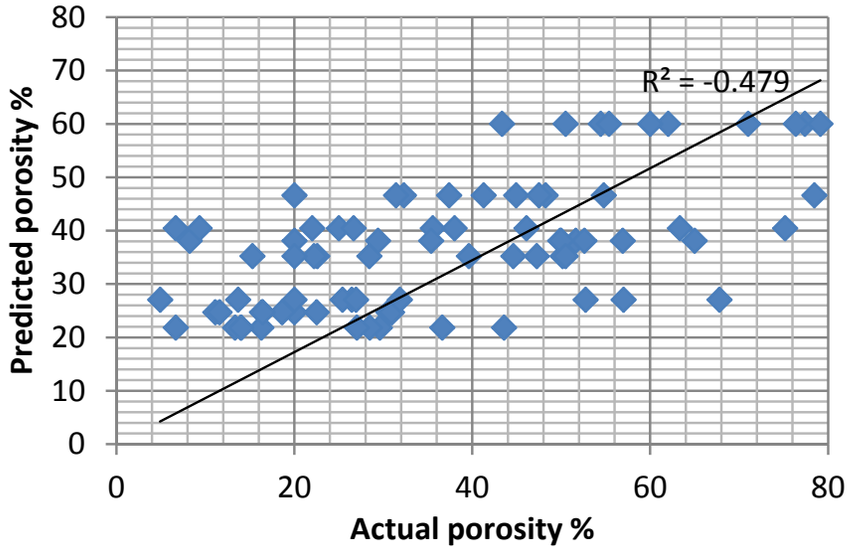


Figure 14. Comparison of experimental and predicted values for porosity content

A study by Azmir and co-authors (2009) developed the first and second order polynomial models of their four factors Taguchi giving to a reasonably high correlation between the actual and predicted values. The coefficients of regression were determined using the same software, Minitab 15. This means this approach could be applicable in this study in order to improve the correlation coefficient of these two models for future work.

3.5. Electrical conductivity

Nickel-YSZ composite is the common material for fuel cell anode and thus the electrical conductivity of this composite fabricated via EN co-deposition process is also investigated. The issue of phosphorus impurity in the EN co-deposit could impede the electronic performance of the composite. The conductivity using four-point probe both in air and nitrogen environment was measured. The air environment is to simulate the oxidation environment and nitrogen for an inert environment. The measured conductivities in different environment were found to be comparable to the published data.

The Ni-YSZ co-deposition was deposited onto a ceramic substrate representing the anode. The initial sample with the thickness of 13 μm Ni-YSZ co-deposition contains 48.32 vol.% Ni. This was co-deposited with 2 μm YSZ particle size. The initial electrical conductivity tests were carried out at room temperature (25^{o}C) and involved measurements at two different points on the surface of the composite sample. The tests were carried out at three different currents- 1mA, 50mA and 100mA. The resistance, resistivity and conductivity of the sample at the three different currents are given in Table 4.

Current	1 mA		50 mA		100 mA	
	1st Point	2nd Point	1st Point	2nd Point	1st Point	2nd Point
Resistance/ Ω	0.117	0.210	0.353	0.425	0.317	0.261
Resistivity/ 10^{-4}Ωcm	1.52	2.73	4.59	5.52	4.12	3.4
Conductivity/10^{4}Scm^{-1}	0.66	0.36	0.22	0.18	0.24	0.29

Table 4. Initial four-point electrical test at various current

The observed values were very encouraging. The initial test was carried out at room temperature using four-point probe measurement. Since YSZ is non-metallic and nickel is metallic, the Ni-YSZ composite behaves as biphasic composite system – having a conductivity percolation threshold at an adequate amount of nickel. The conductivity values of 50 vol.% Ni-YSZ is a factor of ten less than half the value of pure metallic nickel at room temperature (11.8 x10^{4} (Ωcm)$^{-1}$). Thus the obtained values for this initial test are still comparable.

A test on the Ni-YSZ fabricated via EN co-deposition was carried out at temperatures increasing from 25˚C to 420˚C in air. The scatter plot of the resistivity and conductivity are given in Figure 15. The trend of resistivity showed a linear relationship with the temperature. Resistivity increases as temperature increases. The conductivity is inversely proportional to resistivity thus it is expected to show opposite linear relationship to the

resistivity. The linear decrease in conductivity with temperature is indicative of metallic conduction.

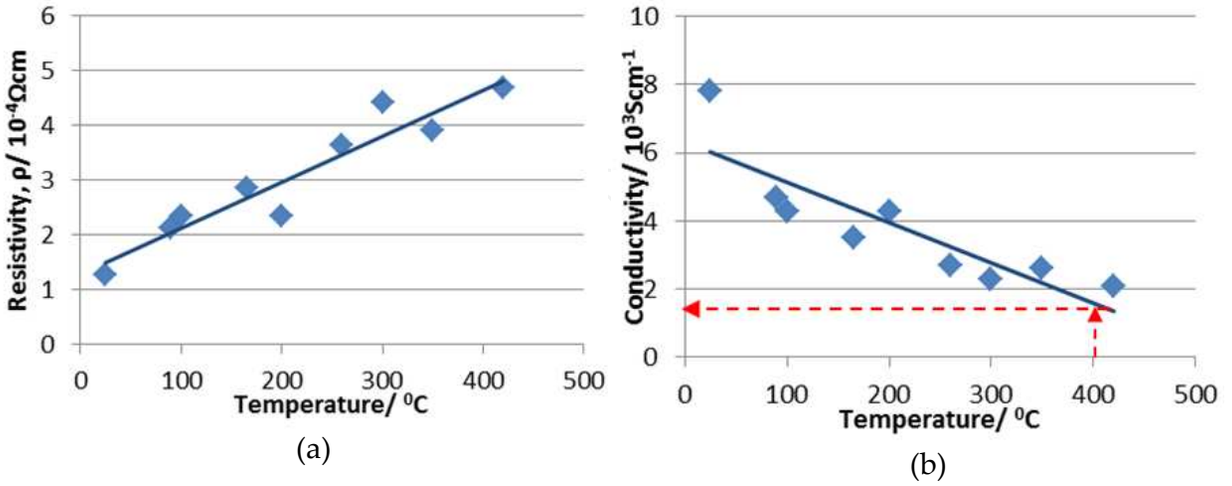


Figure 15. Scatter plot of Ni-YSZ composite (a) resistivity (b) conductivity against temperature in air

This conductivity trend was similar to the study done by Pratihar and co-authors (2005) as shown in Figure 15. The conductivity values obtained from the study at variable fabrication techniques for 40 vol.% Ni at 400⁰C are tabulated in Table 5. Based on the best fitted linear line, at 400°C, the conductivity value of 50 vol.% Ni is approximately 1500 Scm^{-1} (referring to the red dotted line in Figure 15b). This is comparable to the conductivity obtained by the composite fabricated via EN powder coating at 40 vol.% Ni.

Fabrication Technique	σ/ Scm^{-1}
Solid state	450
Liquid dispersion	250
EN powder coating	1100

Table 5. Conductivity values of Ni-YSZ composite fabricated by various techniques at 400°C

A study on a 50 vol.% Ni gave a conductivity of 10 Scm^{-1} (Koide, Someya et al. 2000). Comparing these values with the one obtained for Ni-YSZ composite fabricated via EN coating, the conductivity values for EN co-deposition higher by a factor of hundred. Another study for 50 vol.% Ni-YSZ by Aruna and co-authors (Aruna, Muthuraman et al. 1998) stated a value of 2.5 x 10^3 Scm^{-1} at 400°C which is comparable to the value obtained in this work.

Two series of electrical performance tests were conducted on another Ni-YSZ composite fabricated via EN co-deposition. These were carried out in two different environments – in air varying temperatures from 25°C to 800°C and in nitrogen varying temperatures from 25°C to 600°C. Both composite samples in air and nitrogen had coating deposition thickness of 10 microns. The conductivity plots for both series are given in Figure 16. Again, the conductivity trend decreases with temperature, an indication that it has a metallic conductivity.

The conductivity values are similar in air and nitrogen environment although the former is slightly higher. This observation might be due to the high moisture content in air compared

to nitrogen. A review by Zhu and Deevi (2003) found that the Ni-YSZ composite overpotential is significantly reduced in the presence of moisture or steam. Lowering anodic overpotential enhanced the electronic conductivity.

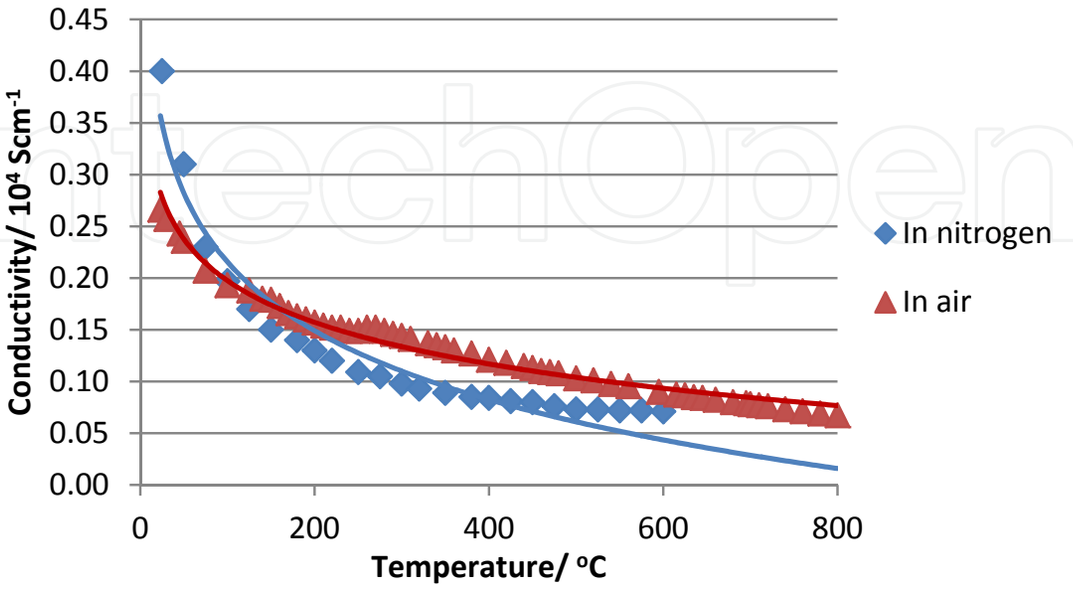


Figure 16. Scatter plot of conductivity against temperature in both nitrogen and air

In general, the conductivity at 600-800°C of Ni-YSZ fabricated via EN deposition ranged between 700-1000 Scm^{-1} in both environments. These values are comparable with the published data from several studies as tabulated in Table 6. The role of phosphorus may be important. Parkinson stated that the electrical resistivity of EN deposited nickel increases with phosphorus content (Parkinson 1997). Referring to the nickel-phosphorus phase diagram, Ni_3P are exists at temperatures greater than 400°C. The effect of these Ni_3P crystals for porosity as it could evaporate at higher temperature in fuel cell anode application should be the subject of future work. For example, this composition might be evaporated at temperature between 1107-1517°C (Viksman and Gordienko 1992).

Composite	T/°C	Fabrication	Environment	σ/ Scm^{-1}	Ref.
40vol.% Ni-YSZ	600	Solid state coating	H_2	1500	Kim et al. (2006)
		Solid state mixing		900	
	800	Solid state coating	H_2	1400	
		Solid state mixing		800	
45wt.% Ni-YSZ	600-800	Solid state with 2-step calcinations	H_2/Ar	500	Han et al. (2006)
		Conventional solid state mixing		430	

Table 6. Published electrical conductivity of Ni-YSZ composite

The composite fabricated via EN co-deposition is a possibility for in-situ fabrication onto ceramic substrate. It is proven the composite of 50 vol.% Ni has a metallic conductivity with

highest conductivity of 1500 Scm^{-1} at 400°C in air and 700 Scm^{-1} in N_2; 1000 Scm^{-1} in air at 600°C and 750 Scm^{-1} at 800°C in air.

4. Conclusions

This study investigates a method of fabricating Ni-YSZ composite via EN co-deposition approach. The work involved (i) showing that successful EN co-deposition of Ni–YSZ composite by selective combinations of process parameters (ii) investigation of physical properties of the composites.

The 2^4 full factorials of 16 runs used particle sizes of 2 and 10 μm, bath agitation methods of air bubbling and mechanical stirring, bath pH of 4.9 and 5.4 and substrate surface treatment of HF etching and mechanical blasting. The design of experiment responses were nickel content and porosity content. The design of experiment were then analysed by Minitab 15 software and it was found that the optimum condition for low Ni to YSZ ratio involved a particle size of 10 μm, bath agitation of mechanical stirring, a bath pH of 4.9 and a substrate condition of HF etching. On the other hand, the porosity response optimum condition involved a particle size of 2 μm, a bath agitation method of mechanical stirring, a bath pH of 4.9 and a substrate surface treatment of mechanical blasting.

Based on the 80 sets of experimental data, the linear regression models were successfully developed for both responses. The coefficients of determinations (R^2) of nickel composition and porosity content were found to be 0.72 and 0.47 respectively. There is a reasonable correlation between the measured values and predicted value for nickel content. These models can be used in determining EN co-deposition parameters for tailored amount of nickel content.

In terms of the electrical conductivity performance, the initial electrical conductivity test carried out at room temperature showed an encouraging outcome in that the value for a 50 vol.% Ni-YSZ composite was only a factor of ten less than the equivalent loading of pure nickel. The electrical conductivity of this composite at 400°C in air was comparable to published data in other studies and was superior to those recorded for composites manufactured by traditional techniques. At temperatures up to 800°C, the electrical conductivity tests were carried out in two different environments - air and nitrogen – and results were comparable to those in the public domain.

Author details

Nor Bahiyah Baba
TATI University College (TATIUC), Terengganu, Malaysia

Acknowledgement

The author would like to express her gratitude to Mr. Alan Davidson and Prof. Tariq Muneer from *School of Engineering and Build Environment, Edinburgh Napier University, United Kingdom* for their technical support and great contribution of knowledge.

5. References

Anthony, J. (2003). *Design of Experiments for Engineers and Scientist*, Butterworth-Henimen.

Apachitei, I., J. Duszczyk, et al. (1998). "Particles Co-Deposition by Electroless Nickel." *Scripta Materialia* 38(9): 1383–1389.

Aruna, S. T., M. Muthuraman, et al. (1998). "Synthesis and properties of Ni-YSZ cermet: anode materials for solid oxide fuel cells." *Solid State Ionics* 111: 45-51.

Azmir, M. A., A. K. Ahsan, et al. (2009). "Effect of abrasive water jet machining parameters on aramid fibre reinforced plastics composite." *International Journal Materials Form* 2: 37-44.

Baba, N. B., W. Waugh, et al. (2009). Manufacture of Electroless Nickel/YSZ Composite Coatings. *World Congress of Science, Engineering and Technology (WCSET)* Dubai, UAE, WASET 2009 ISSN 2070-3740, Vol.37. ISSN 2070-3740, Vol.37: 715-720.

Balaraju, J. N., Kalavati, et al. (2006). "Influence of particle size on the microstructure, hardness and corrosion resistance of electroless Ni–P–Al_2O_3 composite coatings." *Surface & Coatings Technology* 200: 3933 – 3941.

Balaraju, J. N., T. S. N. S. Narayanan, et al. (2006). "Structure and phase transformation behaviour of electroless Ni–P composite coatings." *Materials Research Bulletin* 41: 847–860.

Balaraju, J. N. and K. S. Rajam (2008). "Preparation and characterisation of sutocatalytic low phosphorus nickel coatings containing submicron nitride particles." *Journal of Alloys and Compounds* 459(1-2): 311–319.

Baudrand, D. W. (1994). "Electroless Nickel Plating " *ASM Handbook Volume 5* Surface Engineering: 290-310.

Berkh, S. Eskin, et al. (March 1996). Properties of Electrodeposited NiP-SiC Composite Coatings. *Metal Finishing*: 35-40.

Bisgaard, S. (1998). A Practical Aid for Experimenters. *Preliminary Edition*. Madison, Starlight Press: 57.

Dai, J., X. Liu, et al. (2009). "Preparation of Ni-coated Si_3N_4 powders via electroless plating method." *Ceramics International* 35(8): 3407–3410.

Das, C. M., P. K. Limaye, et al. (2007). "Preparation and characterization of silicon nitride codeposited electroless nickel composite coatings." *Journal of Alloys and Compounds* 436: 328-334.

Das, L. and D. T. Chin (1959). "Electrochemical Porosity Measurement of EN Coating." *Plating and Surface Finishing* 84: 66-68.

Dong, D., X. H. Chen, et al. (2009). "Preparation and properties of electroless Ni-P-SiO_2 composite coatings." *Applied Surface Science* 255: 7051-7055.

Feldstein, N. (1990). Composites Electroless Plating. *Electroless Plating: Fundamentals and Applications*. G. O. Mallory and J. B. Hajdy. Orlondo, FI, AESF Publication. Chapter 11: 269-287.

Gengler, J. J., C. Muratore, et al. (2010). "Yttria-stabilized zirconia-based composites with adaptive thermal conductivity " *Composites Science and Technology* 70(14): 2117-2122.

Ger, M.-D. and B. J. Hwang (2002). "Effect of surfactants on codeposition of PTFE particles with electroless Ni-P coating." *Materials Chemistry and Physics* 76(1): 38-45.

Han, K. R., Y. Jeong, et al. (2006). "Fabrication of NiO/YSZ anode material for SOFC via mixed NiO precursors." *Materials Letters* 61: 1242–1245.

Hazan, Y. d., T. Reutera, et al. (2008). "Interactions and dispersion stability of aluminum oxide colloidal particles in electroless nickel solutions in the presence of comb polyelectrolytes." *Journal of Colloid and Interface Science* 323: 293–300.

Hazan, Y. d., D. Werner, et al. (2008). "Homogeneous Ni-P/Al_2O_3 nanocomposite coatings from stable dispersions in electroless nickel baths." *Journal of Colloid and Interface Science* 328: 103–109.

Huang, Y. S., X. T. Zeng, et al. (2003). "Development of electroless Ni-P-PTFE-SiC composite coating." *Surface & Coating Technology* 167: 207-211.

Hung, C. C., C. C. Lin, et al. (2008). "Tribological studies of electroless nickel/ diamond composite coatings on steels." *Diamond & Related Materials* 17: 853–859.

Kalantary, M. R., K. A. Holbrook, et al. (1993). "Optimisation of a Bath for Electroless Plating and its use for the Production of Ni-P-SiC Coatings." *Trans. Inst. Metal Finish* 71(2): 55-61.

Kim, S.-D., H. Moon, et al. (2006). "Performance and durability of Ni-coated YSZ anodes for intermediate temperature solid oxide fuel cells." *Solid State Ionics* 177: 931-938.

Koide, H., Y. Someya, et al. (2000). "Properties of Ni/YSZ cermet as anode for SOFC." *Solid State Ionics* 132: 253-260.

Lekka, M., C. Zanella, et al. (2010). "Scaling-up of the electrodeposition process of nano-composite coating for corrosion and wear protection " *Electrochimica Acta* 55(27): 7876-7883.

Li, L., M. An, et al. (2005). "Model of electroless Ni deposition on SiC_p/Al composites and study of the interfacial interaction of coatings with substrate surface." *Applied Surface Science* 252: 959-965.

Li, L., M. An, et al. (2006). "A new electroless nickel deposition technique to metallise SiC_p/Al composites." *Surface & Coatings Technology* 200: 5102 – 5112.

Li, L. B., M. Z. An, et al. (2005). "Electroless deposition of nickel on the surface of silicon carbide/aluminum composites in alkaline bath." *Materials Chemistry and Physics* 94: 159-164.

Li, Y. (1997). Investigation of Electroless Ni-P-SiC Composite Coatings. *Plating & Surface Finishing*. November 1997: 77-81.

Lin, C. J., K. C. Chen, et al. (2006). "The cavitation erosion behavior of electroless Ni–P–SiC composite coating." *Wear* 261: 1390–1396.

Liu, W. L., S. H. Hsieh, et al. (2006). "Temperature and pH dependence of the Electroless Ni-P deposition on Silicon." *Thin Solid Films* 510: 102 – 106.

Matsubara, H., Y. Abe, et al. (2007). "Co-deposition mechanisms of nano-diamond with electrolessly plated nickel films." *Electrochimica Acta* 52: 3047-3052.

McCormack, A. G., M. J. Pomeroy, et al. (2003). *Journal of Electrochemical Society* 150 (5): C356-C361.

Necula, B. S., I. Apachitei, et al. (2007). "Stability of nano-/microsized particles in deionized water and electroless nickel solutions." *Journal of Colloid and Interface Science* 314: 514–522.

Parkinson, R. (1997). Properties and Application of Electroless Nickel, Nickel Development Institute: 33.

Periene, N., A. Cesuniene, et al. (1994). Codeposition of Mixtures of Dispersed Particles With Nickel-Phosphorus Electrodeposits. *Plating ans Surface Finishing*. October 1994: 68-71.

Pratihar, S. K., A. D. Sharma, et al. (2005). "Processing microstructure property correlation of porous Ni–YSZ cermets anode for SOFC application." *Materials Research Bulletin* 40: 1936–1944.

Pratihar, S. K., A. D. Sharma, et al. (2007). "Properties of Ni/YSZ porous cermets prepared by electroless coating technique for SOFC anode application." *Journal of Materials Science* 42: 7220-7226.

Rabizadeh, T. and S. R. Allahkaram (2011). "Corrosion resistance enhancement of Ni–P electroless coatings by incorporation of nano-SiO_2 particles." *Materials and Design* 32(1): 133-138.

Sartorius (1991). Manual of weighing applications Part 1: Density: 1-62.

Schloetter (2006). Electroless Nickel - Solotonip 1850. *Bath 18810 - PE*. Worchestershire, England: 1-11.

Sevugan, K., M. Selvam, et al. (1993). Effect of Agitation in Electroless Nickel Deposition. *Plating and Surface Finishing*: 56-58.

Sharma, S. B., R. C. Agarwala, et al. (2005). "Development of Electroless Composite Coatings by using in-situ Co-deposition followed by co-deposition process." *Sadhana* 28: 475–493.

Sheela, G. and M. Pushpavanam (2002). Diamond-dispersed electroless nickel coatings. *Metal finishing*. January 2002: 45-47.

Shibli, S. M. A., V. S. Dilimon, et al. (2006). "ZrO_2-reinforced Ni–P plate: An effective catalytic surface for hydrogen evolution." *Applied Surface Science* 253: 2189–2195.

Simwonis, D., H. Thulen, et al. (1999). "Properties of Ni/YSZ porous cermets for SOFC anode substrates prepared by tape casting and coat-mix process." *Journal of Materials Processing Technology* 92-93: 107-111.

Taheri, R., I. N. A. Oguocha, et al. (2001). "The tribological characteristics of electroless NiP coatings." *Wear* 249: 389–396.

Teixeira, L. A. C. and M. C. Santini (2005). "Surface Conditioning of ABS for Metallisation into the use of Chromium baths." *Journal of Materials Processing Technology* 170: 37–41.

Vaghefi, S. M. M., A. Saatchi, et al. (2003). "Deposition and properties of electroless Ni-P-B_4C composite coatings." *Surface and Coatings Technology* 168: 259-262.

Vaghefi, S. M. M., A. Saatchi, et al. (1997). "The effect of agitation on electroless nickel-phosphorus-molybdenum disulfide composite plating." *Metal Finishing* 95(6): 102.

Viksman, G. S. and S. P. Gordienko (1992). "Behavior in vacuum at high temperatures and thermodynamic properties of nickel phosphide Ni_3P." *Poroshkovskaya Metallurgiya* 12(360): 70-72.

Wang, L., Y. Wang, et al. (2011). "Influence of pores on the thermal insulation behavior of thermal barrier coatings prepared by atmospheric plasma spray " *Materials and Design* 32(1): 36-47.

Wang, Y., M. E. Walter, et al. (2006). "Effects of powder sizes and reduction parameters on the strength of Ni–YSZ anodes." *Solid State Ionics* 177: 1517-1527.

Wu, Y., B. Shen, et al. (2006). "The tribological behaviour of electroless Ni–P–Gr–SiC composite." *Wear* 261: 201–207.

Zhu, W. Z. and S. C. Deevi (2003). "A review on the status of anode materials for solid oxide fuel cells." *Materials Science and Engineering* A362: 228-239.

Zuleta, A. A., O. A. Galvis, et al. (2009). "Preparation and characterization of electroless Ni–P–Fe_3O_4 composite coatings and evaluation of its high temperature oxidation behaviour." *Surface & Coatings Technology* 203: 3569–3578.

IntechOpen